

Two-neutron halo structure and anti-halo effect in ^{31}F

Hiroshi Masui · Wataru Horiuchi ·
Masaaki Kimura

Received: date / Accepted: date

Abstract We perform a detailed analysis for the structure of ^{31}F , which is a candidate of the halo nucleus. We calculate the radius and reaction cross-section using a three-body model of $^{29}\text{F}+n+n$ and discuss how the competition between the neutron-pairing and the single-particle energy induces structural changes of ^{31}F . The present analysis further clarifies a new aspect of the anti-halo effect that suppresses the halo structure.

1 Introduction

Characteristic nuclear structure with loosely bound nucleons is called “halo” and has been extensively studied from both the theoretical and experimental sides [1, 2]. In recent years, a drip-line nucleus of the fluorine isotopes ^{31}F has been observed [3]. Because of the small neutron separation energy and the subsystem ^{30}F ($^{29}\text{F}+n$) being unbound, ^{31}F is expected to have a halo structure same as other Borromean nuclei, e.g. ^6He , ^{11}Li , ^{14}Be , and ^{19}B . On the other hand, although development of the halo structure is closely related to the small neutron separation energy, a mechanism to suppress the nuclear radius in weakly bound systems has been discussed as the “pairing anti-halo” effect [4, 5].

Therefore, in order to give a theoretical prediction to the structure of ^{31}F , we performed three-body calculations using a $^{29}\text{F}+n+n$ model and showed the matter radius and reaction cross-sections of ^{31}F in Ref. [6]. This analysis revealed that the gap between the p -orbit and f -orbit in the subsystem ^{30}F is the essential ingredient

H. Masui
Information Processing Center, Kitami Institute of Technology, Kitami, 090-8507, Japan
E-mail: hgmasui@mail.kitami-it.ac.jp

W. Horiuchi
Department of Physics, Hokkaido University, Sapporo 060-0810, Japan

M. Kimura
Department of Physics, Hokkaido University, Sapporo 060-0810, Japan and
Nuclear Reaction Data Centre, Hokkaido University, Sapporo 060-0810, Japan and
Research Center for Nuclear Physics (RCNP), Osaka University, Ibaraki, 567-0047, Japan

to determine the radius of ^{31}F . Furthermore, a new aspect to the anti-halo effect was proposed.

In this paper, we discuss the mechanism of the newly proposed anti-halo effect of ^{31}F more detail and clarify a general condition for the formation of the halo structure and the occurrence of the anti-halo effect.

2 Theoretical model and interactions

We calculate the structure of ^{31}F in a $^{29}\text{F}+n+n$ three-body model. To describe ^{31}F as a loosely-bound Borromean system, the calculation method is required to be able to accurately take into account the continuum states. For this purpose, we employ the cluster-orbital shell model (COSM) [7] with the Gaussian expansion method (GEM) [8,9].

The Hamiltonian and basis functions in COSM with GEM for the $^{29}\text{F}+n+n$ system are briefly explained below. The Hamiltonian by removing the center of mass motion in COSM is formulated as follows:

$$\hat{H} = \sum_{i=1}^2 (\hat{T}_i + \hat{V}_i + \lambda \hat{A}_i) + (\hat{t}_{12} + \hat{v}_{12}). \quad (1)$$

Here, $\lambda \hat{A}$ is introduced to eliminate the Pauli forbidden states in the procedure of the orthogonality condition model [10], and \hat{t}_{12} is the recoil term induced by the subtraction of the center of mass motion.

We solve the eigenvectors of the Hamiltonian (1) using the Gaussian basis $\Phi_{pq\ell j}^{JM}$ in a variational way as $\Psi_{JM} = \sum_{pq\ell j} C_{pq\ell j} \Phi_{pq\ell j}^{JM}$. Since we assume the core nucleus ^{29}F as a spin-less particle for simplicity, the spin-parity of ^{31}F is determined by the valence nucleons part $\Phi_{pq\ell j}^{JM} \equiv \mathcal{A}\{[\phi_{p\ell j}(1) \otimes \phi_{q\ell j}(2)]_{JM}\}$. For the basis functions, we take the maximum orbital angular momentum up to 5, and the width parameters of the Gaussian are prepared using a geometric progression manner, where 20 bases are applied for each coordinate. Therefore, for example, a typical basis size is 2310 for the 0^+ state.

For the $^{29}\text{F}+n$ interaction \hat{V}_i , we employ the Woods-Saxon (WS) potential using the same parameter sets for reproducing the reaction cross-sections of ^{31}Ne [11], which is the next nucleus of ^{30}F by a proton. Since there is no information other than ^{30}F being unbound, we adjust the strength parameter V_0 using two different values for each set of $\{r_0, a\}$ in WS under the condition that ^{30}F is unbound and ^{31}Ne is bound. This leads to 12 different parameter sets for the calculation [6]. For the neutron-neutron potential \hat{v}_{12} , we use the central part of the Minnesota potential [12] with the exchange parameter $u = 1.0$.

3 Results and Discussion

First, we perform calculations using the 12 different parameter sets. As a result, the two-neutron separation energies S_{2n} are obtained in the range of 0.44 – 1.37 MeV, and the matter radius R_{rms} varies in the range of 3.48 – 3.70 fm. For the maximum radius case $R_{\text{rms}} = 3.70$ fm, the halo structure is considered to be well developed. We also calculate the reaction cross-sections at the incident energies 240

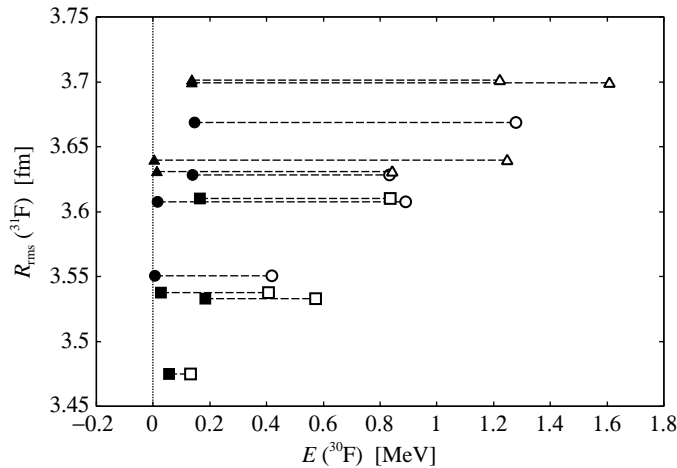


Fig. 1 Calculated matter radius of ^{31}F in different parameter sets of $\{V_0, a, r_0\}$ with the WS potential of ^{30}F . The x -axis shows the energy of ^{30}F , and the triangles, circles and squares are the results for the parameter sets of $r_0 = 0.65, 0.70,$ and 0.75 fm, respectively. Dashed-line indicates the pair of ^{30}F energies for $p_{3/2}$ (solid) and $f_{7/2}$ (open) orbits. For detail, see text.

and 900 MeV/nucleon using the Glauber model (NTG) [13, 14, 15, 16] and obtain large cross-sections as 1530 and 1640 mb [6]. This result further supports the large matter radius of ^{31}F , i.e. the halo structure, is realized under a certain condition in ^{30}F .

Next, to clarify the condition, we analyze the characteristics of the results for ^{31}F using the 12 parameter sets. To this end, we introduce the Pearson's correlation coefficient (PCC) between two variables x and y ,

$$r_{xy} = \frac{\sum_{i=1}^M (x_i - \bar{x})(y_i - \bar{y})}{\{\sum_{i=1}^M (x_i - \bar{x})^2\}^{1/2} \{\sum_{i=1}^M (y_i - \bar{y})^2\}^{1/2}}. \quad (2)$$

Contrary to an expectation from the standard picture that a small binding energy leads to a large nuclear radius due to the extension of the wave function in the asymptotic region, the obtained correlation between S_{2n} and R_{rms} becomes not so strong, i.e. $r_{xy} = -0.801$. Therefore, a question arises, “which physical quantity is the explanatory variable to determine the nuclear radius?”

To answer this question, we plot the calculated results of the 12 parameter sets in Fig. 1 under the following manner. We take the x -axis for the energies of the p -orbit and the f -orbit in ^{30}F and the y -axis for the matter radius of ^{31}F . The symbols are assigned to different diffuseness parameters as $a = 0.65, 0.70,$ and 0.75 fm, and the distance between the solid and open symbols connected by a dashed-line corresponds to the energy gap between the $p_{3/2}$ orbit and the $f_{7/2}$ orbit in ^{30}F . As seen from Fig. 1, it can be considered that the radius of ^{31}F is strongly correlated to the energy gap in ^{30}F .

In order to confirm the above investigation, we calculate PCC between the energy gap $\Delta\varepsilon$ in ^{30}F and the radius R_{rms} of ^{31}F . Here, the energy gap is defined as $\Delta\varepsilon \equiv \varepsilon(f) - \varepsilon(p)$, where $\varepsilon(f)$ and $\varepsilon(p)$ are the real part of the resonant energies of the lowest orbits of $7/2^-$ and $3/2^-$ in ^{30}F , respectively. The obtained PCC

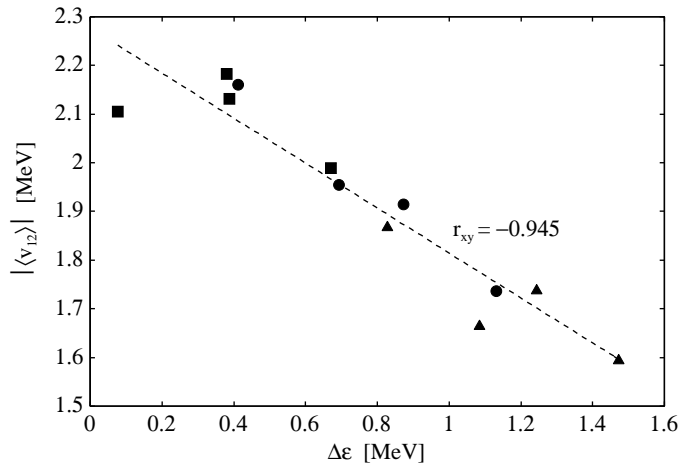


Fig. 2 The correlation between the absolute value of the neutron-neutron interaction $\langle \hat{v}_{12} \rangle$ in the ${}^{31}\text{F}$ system and the energy gap $\Delta\epsilon$ in ${}^{30}\text{F}$. The definition of the triangles, circles and squares are the same with those applied in Fig. 1.

shows very strong correlation as $r_{xy} = 0.935$, which is stronger than that obtained for S_{2n} and R_{rms} as $r_{xy} = -0.801$. Therefore, we consider the energy gap $\Delta\epsilon$ is a key variable to indicate the structural change of ${}^{31}\text{F}$.

The energy gap also has a close relationship to the expectation value of the neutron numbers for the valence orbits in ${}^{31}\text{F}$. We calculate these numbers for the $p_{3/2}$ orbit ($N(p)$) and the $f_{7/2}$ orbit ($N(f)$), where $N(f)$ and $N(p)$ are added up to 2 including other orbits. In the largest radius case $R_{\text{rms}} = 3.70$ fm, $N(p)$ and $N(f)$ are obtained as 1.63 and 0.19, respectively, i.e. ${}^{31}\text{F}$ is p -wave dominant. On the other hand, in the smallest radius case $R_{\text{rms}} = 3.48$ fm, ${}^{31}\text{F}$ becomes f -wave dominant as $N(p) = 0.38$ and $N(f) = 1.53$. As shown in Fig. 3 of Ref. [6], $N(p)$ and $N(f)$ change inseparably and intersect each other at about $\Delta\epsilon = 0.4$ MeV. Hence, it is confirmed that the energy gap $\Delta\epsilon$ is related to the neutron numbers and also to the radius. However, even in the smallest radius case, a small separation energy $S_{2n} = 1.37$ MeV leads to the small radius $R_{\text{rms}} = 3.48$ fm. Therefore, we consider a new mechanism to shrink the nuclear radius should occur in ${}^{31}\text{F}$, which can be an “anti-halo” effect.

Next, we investigate how the energy gap affects to the pairing strength in the Borromean system, since the anti-halo effect has been discussed in terms of the pairing correlation [4,5]. Figure 2 shows the absolute value of $\langle \hat{v}_{12} \rangle$ in the Hamiltonian (1) with respect to the change of the energy gap $\Delta\epsilon$. As shown in Fig. 2, $\Delta\epsilon$ is strongly correlated to $|\langle \hat{v}_{12} \rangle|$, where PCC is obtained as $r_{xy} = -0.945$. It is noted that the correlation between the separation energy S_{2n} and $|\langle \hat{v}_{12} \rangle|$ is very weak by considering PCC obtained as $r_{xy} = 0.660$. Combined with the result for the $\Delta\epsilon$ dependence of $N(p)$ and $N(f)$, we can confirm that $|\langle \hat{v}_{12} \rangle|$, which can be an index of the neutron-neutron correlation, increases for a small energy gap, and ${}^{31}\text{F}$ becomes f -wave dominant. As a result, the radius of ${}^{31}\text{F}$ shrinks even though the separation energy is still small.

To realize the strong correlations between $\Delta\epsilon$ and other quantities such as R_{rms} , $N(p)$, $N(f)$, and $|\langle \hat{v}_{12} \rangle|$, and the shrinkage of the radius induced by $\Delta\epsilon$,

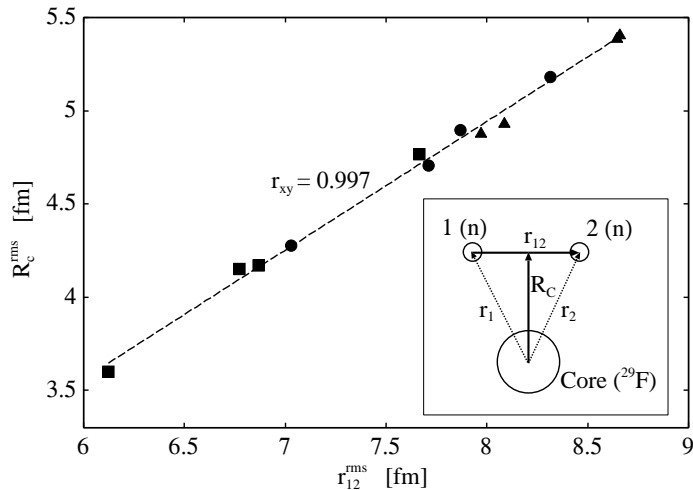


Fig. 3 The correlation between $r_{12}^{\text{rms}} \equiv \sqrt{\langle r_{12}^2 \rangle}$ and $R_c^{\text{rms}} \equiv \sqrt{\langle R_c^2 \rangle}$. The right-bottom panel shows the coordinate system of the $^{29}\text{F}+n+n$ three-body system in COSM (r_1 and r_2), and the definition of r_{12} and R_c . The definition of the triangles, circles and squares are the same with those applied in Fig. 1.

there is another important condition that is the inversion of the valence orbits. ^{30}F and ^{31}F are considered to be placed on the “island of inversion”, where the order of the single-particle orbits is inverted from the normal shell-model one. If the f -orbit ($f_{7/2}$) lies above the p -orbit ($p_{3/2}$), a competition occurs between the energy loss from the gap $\Delta\varepsilon$ and the gain from the nucleon-nucleon interaction $|\langle \hat{v}_{12} \rangle|$, and consequently, $\Delta\varepsilon$ becomes an explanatory variable to determine $|\langle \hat{v}_{12} \rangle|$, $N(f)$, $N(p)$, and R_{rms} .

From the above discussion, the key ingredient that determines the nuclear radius of ^{31}F is considered to be the energy gap between the $p_{3/2}$ orbit and the $f_{7/2}$ orbit in ^{30}F . The formation of the halo structure in ^{31}F depends on whether the energy gap is large enough to overcome the energy loss of the nucleon-nucleon interaction part. Such the situation generally occurs for systems that the valence particle orbitals are inverted, i.e. a smaller angular momentum orbit lies below a higher angular momentum orbit. As the energy gap decreases, neutrons begin to occupy the orbit with the higher angular momentum, and the nucleon-nucleon interaction part gives larger contribution to overcome the energy loss from the gap. As a result, the radius becomes small even for a small separation energy. We consider this mechanism is a novel anti-halo effect.

Finally, in addition to the anti-halo effect, we investigate the possibility of the di-neutron like localization in ^{31}F . The correlation between the neutron-neutron distance $r_{12}^{\text{rms}} \equiv \sqrt{\langle r_{12}^2 \rangle}$ and distance from the core to the center of mass of valence neutrons $R_c^{\text{rms}} \equiv \sqrt{\langle R_c^2 \rangle}$ is shown in Fig. 3. If the ratio of r_{12}^{rms} to R_c^{rms} deviates from the line, for example, in the case of a small r_{12}^{rms} and a large R_c^{rms} , the neutrons are supposed to have a di-neutron like localization. However, the correlation becomes very strong as $r_{xy} = 0.997$, which is almost the liner correlation, and it is difficult to find a possibility of the di-neutron like localization for the parameter sets of this calculation.

4 Summary

We study the structure of ^{31}F , which is the drip-line nucleus of the fluorine isotopes, using COSM with GEM in a $^{29}\text{F}+n+n$ three-body model. Since there is an ambiguity to determine the $^{29}\text{F}+n$ potential, the strength parameter of WS can be changed by keeping the consistency for ^{31}Ne and ^{30}F . The correlation analysis is performed from the results using the 12 different parameter sets by keeping the consistency. As a result, we found that the key ingredient to determine the nuclear radius of ^{31}F is the energy gap between the $p_{3/2}$ orbit and $f_{7/2}$ orbit in ^{30}F . This is considered as a general condition for other nuclei near the drip-line, where the valence orbits are inverted, and it is expected that the cross over of the halo structure and the occurrence of the anti-halo effect can be determined by the energy gap between these inverted valence orbits.

Acknowledgements This work was in part supported by JSPS KAKENHI Grant Nos. 18K03636, 18K03635, 18H04569, 19H05140, and 19K03859, and the collaborative research program 2021, information initiative center, Hokkaido University.

References

1. I. Tanihata, H. Savajols, and R. Kanungo, Recent experimental progress in nuclear halo structure studies, *Prog. Part. Nucl. Phys.* **68**, 215 (2013).
2. M. V. Zhukov, B. V. Danilin, D. V. Fedorov, J. M. Bang, I. J. Thompson, J. S. Vaagen, Bound state properties of Borromean halo nuclei: ^6He and ^{11}Li , *Phys. Rep.* **231**, 151 (1993).
3. D. S. Ahn, N. Fukuda, H. Geissel, N. Inabe, N. Iwasa, T. Kubo *et al.*, Location of the neutron dripline at fluorine and neon, *Phys. Rev. Lett.* **123**, 212501 (2019).
4. K. Bennaceur, J. Dobaczewski, and M. Płoszajczak, Pairing anti-halo effect, *Phys. Lett. B* **496**, 154 (2000).
5. K. Hagino and H. Sagawa, Evidence for a pairing anti-halo effect in the odd-even staggering in reaction cross sections of weakly bound nuclei, *Phys. Rev. C* **84**, 011303(R) (2011).
6. H. Masui, W. Horiuchi, M. Kimura, Two-neutron halo structure of ^{31}F and a novel pairing antihalo effect, *Phys. Rev. C* **101**, 041303(R) (2020).
7. Y. Suzuki and K. Ikeda, Cluster-orbital shell model and its application to the He isotopes, *Phys. Rev. C* **38**, 410 (1988).
8. T. Myo, Y. Kikuchi, H. Masui, and K. Katō, Recent development of complex scaling method for many-body resonances and continua in light nuclei, *Prog. Part. Nucl. Phys.* **79**, 1 (2014).
9. H. Masui, K. Katō, N. Michel, and M. Płoszajczak, Precise comparison of the Gaussian expansion method and the Gamow shell model, *Phys. Rev. C* **89**, 044317 (2014).
10. S. Saito, Theory of Resonating Group Method and Generator Coordinate Method and Orthogonality Condition Model, *Prog. Theor. Phys. Suppl.* **62**, 11 (1977).
11. W. Horiuchi, Y. Suzuki, P. Capel, and D. Baye, Probing the weakly-bound neutron orbit of ^{31}Ne with total reaction and one-neutron removal cross sections, *Phys. Rev. C* **81**, 024606 (2010).
12. D. R. Thompson, M. LeMere, and Y. C. Tang, Systematic investigation of scattering problems with the resonating-group method, *Nucl. Phys. A* **286**, 53 (1977).
13. R. J. Glauber, *Lectures in Theoretical Physics*, edited by W. E. Brittin and L. G. Dunham (Interscience, New York, 1959), Vol. 1, p. 315.
14. B. Abu-Ibrahim and Y. Suzuki, Utility of nucleon-target profile function in cross section calculations, *Phys. Rev. C* **61**, 051601(R) (2000).
15. B. Abu-Ibrahim, W. Horiuchi, A. Kohama, and Y. Suzuki, Reaction cross sections of carbon isotopes incident on a proton, *Phys. Rev. C* **77**, 034607 (2008); **80**, 029903(E) (2009); **81**, 019901(E) (2010).
16. W. Horiuchi, T. Inakura, T. Nakatsukasa, and Y. Suzuki, Glauber-model analysis of total reaction cross sections for Ne, Mg, Si, and S isotopes with Skyrme-Hartree-Fock densities, *Phys. Rev. C* **86**, 024614 (2012).